Volume 5, Issue 2

Malaysia Journal of Invention and Innovation

https://journal.academicapress.org/aps/index.php/mjii

Research Article

PULSE (Predictive Utility for Learning Systems in Evaluating Anemia and Hypertension): A Photoplethysmography (PPG) And Machine Learning–Based Device for Non-Invasive Monitoring of Hb, HR, SpO2, and BP

Jeza Maristel Abanes[1,*], Angelo Jacob Castillo[2], Venisse Kyle Claudio[3], Jazz Gatinao[4], and Althea Sales[5]

1 Tupi National High School; jezamaristel01@gmail.com
2 Tupi National High School; angelojacobdc@gmail.com
3 Tupi National High School; venisseclaudio607@gmail.com
4 Tupi National High School; gatinaojazz@gmail.com
5 Tupi National High School; altheasales882@gmail.com
* Correspondence: Venisse Kyle V. Claudio; +639631821030

Keywords:
Anemia
Hypertension
Photoplethysmography
Non-Invasive Screening
Portable Health Device

Abstract: *Anemia and hypertension remain prevalent health concerns in low-resource communities with limited diagnostic access. This study developed PULSE, a portable, non-invasive screening device using photoplethysmography and multiple linear regression to estimate hemoglobin, blood pressure, oxygen saturation, and heart rate in real time. PULSE was validated against standard clinical instruments. Results showed no significant differences ($p > 0.05$) between PULSE and reference devices. The MLR model achieved $R^2 = 0.972$, RMSE = 2.18, MAE = 1.60, and MAPE = 1.45% for hemoglobin prediction. Blood pressure estimation attained $R^2 = 0.97$ (SBP) and $R^2 = 0.95$ (DBP) with mean errors of 2.4 mmHg and 2.7 mmHg. Strong correlations ($r = 0.951–0.984$) and ICC = 0.981 confirmed high reliability. The system displayed results within 1.82 s (OLED) and 2.14 s (Wi-Fi) with 100% logging accuracy and 93.3% mapping precision. These findings confirm that PULSE is a reliable, accurate, and cost-effective solution for early anemia and hypertension screening.*

1. INTRODUCTION

Anemia and hypertension remain critical global health burdens, disproportionately affecting low- and middle-income countries. Anemia, characterized by reduced hemoglobin or red blood cells, impairs oxygen transport and contributes to fatigue, cognitive deficits, and increased infection risk. The World Health Organization (2023) estimates that anemia affects 40% of children aged 6–59 months, 37%

of pregnant women, and 30% of women of reproductive age worldwide. From 1990 to 2019, more than 1.8 billion individuals across 204 countries were affected, with the highest burden among children and women of reproductive age (Gardner & Kassebaum, 2020). Iron-deficiency anemia remains predominant in resource-limited settings (Safiri et al., 2021).

Hypertension, defined as persistently elevated blood pressure, affects 1.28 billion adults aged 30–79 years globally, nearly two-thirds residing in low- and middle-income countries (World Health Organization, 2023). Although often asymptomatic, it is a major risk factor for cardiovascular disease, stroke, and renal failure (Kario, 2018). Its increasing prevalence is associated with aging populations, urbanization, unhealthy diets, and physical inactivity (Gupta et al., 2019). The coexistence of anemia and hypertension compounds cardiovascular risk, underscoring the importance of integrated screening strategies (Hasan et al., 2018).

In the Philippines, anemia affects 32.4% of children aged 0–5 years and 30% of school-aged children (FNRI-DOST, 2019), while hypertension incidence continues to rise, particularly in rural communities with limited healthcare access (Department of Health, 2022; Goyena et al., 2020). In Mindanao and South Cotabato, food insecurity, recurrent droughts, and soil-transmitted helminth infections (10–20% prevalence among school-aged children) further increase vulnerability (UNICEF, 2022; Delgado et al., 2021). High rates of undiagnosed hypertension reflect gaps in routine screening and primary care (Torres & Cruz, 2020).

Despite their prevalence, rural diagnosis remains constrained. Hemoglobin assessment requires invasive laboratory procedures, and blood pressure monitoring depends on cuff-based devices often unavailable in remote schools and barangay health centers, leading to delayed detection and preventable complications (Santos et al., 2019; Hasan et al., 2018). These limitations highlight the need for portable, non-invasive, and community-deployable screening technologies.

PULSE addresses this gap by providing Wi-Fi- and GPS-enabled, real-time, geotagged screening for anemia and hypertension in schools and barangay health stations. By enabling early detection and community-level monitoring, the system supports timely intervention in high-risk areas and aligns with SDG 3 (Good Health and Well-being), SDG 1 (No Poverty), and SDG 10 (Reduced Inequalities). Through multi-parameter sensing and real-time analytics, PULSE offers a cost-effective approach to improving preventive healthcare access in resource-limited communities.

This study develops and evaluates PULSE (Predictive Utility for Learning Systems in Evaluating Anemia and Hypertension), a portable, non-invasive hemoglobin and vital signs screening device using Photoplethysmography (PPG) technology. It includes a website for real-time data display, logging, and health mapping. Specifically, the objectives of this research are as follows:

1. Evaluate the accuracy of the Multiple Linear Regression (MLR) model of the PULSE system in predicting hemoglobin levels, using performance metrics such as:
    1.1. R-squared (Coefficient of Determination);
    1.2. Root-Mean Square Error (RMSE);
    1.3. Mean Absolute Error (MAE);
    1.4. Mean Absolute Percentage Error (MAPE)?
2. Analyze the relationship between hemoglobin measurements obtained using different methods and the accuracy of the PULSE system, specifically:
    2.1. Determine if there is a significant difference between manual and machine-based hemoglobin measurements.

2.2. Assess if there is a significant difference between machine-based measurements and the PULSE system.

2.3. Evaluate any significant difference between manual hemoglobin measurement and the PULSE system.

3. Determine the accuracy of the PULSE system in predicting Systolic Blood Pressure (SBP) and Diastolic Blood Pressure (DBP) using Photoplethysmography (PPG)-derived parameters. Specifically:

    3.1. The accuracy of the Multiple Linear Regression (MLR) model of the PULSE system in estimating SBP is evaluated based on the following performance metrics:

        3.1.1. R-squared (Coefficient of Determination);

        3.1.2. Root-Mean Square Error (RMSE);

        3.1.3. Mean Absolute Error (MAE);

        3.1.4. Mean Absolute Percentage Error (MAPE).

    3.2. The accuracy of the Multiple Linear Regression (MLR) model of the PULSE system in estimating DBP is evaluated using the following performance metrics:

        3.2.1. R-squared (Coefficient of Determination);

        3.2.2. Root-Mean Square Error (RMSE);

        3.2.3. Mean Absolute Error (MAE);

        3.2.4. Mean Absolute Percentage Error (MAPE).

4. The significance of the difference between blood pressure (BP) measurements obtained using a sphygmomanometer and those estimated by the PULSE system is evaluated.

5. The accuracy of the PULSE system in measuring SpO_2 status and heart rate level is evaluated in comparison with clinically accepted normal ranges. Specifically:

    5.1. The significance of the difference between the SpO_2 status measured by the PULSE system and that measured by a commercial pulse oximeter is evaluated.

    5.2. The significance of the difference between the heart rate level measured by the PULSE system and that measured by a commercial pulse oximeter is evaluated.

6. The mean response time (in seconds) of the PULSE system after a successful health scan is measured in terms of:

    6.1. via Wi-Fi to the website;

    6.2. display on the built-in OLED screen.

7. Develop a web-based platform that integrates and visualizes the results of the Multiple Linear Regression (MLR) model from the PULSE system to enable real-time health monitoring and efficient data management.

8. Design a Wi-Fi–enabled website that performs effectively under real-time conditions in terms of:

8.1. accuracy of data logging

8.2. functionality of health mapping display.

9. Meet the integration requirements of the PULSE system in terms of;

9.1. accuracy;

9.2. functionality;

9.3. acceptability.

2. LITERATURE REVIEW

4.1. Anemia

Anemia, characterized by reduced hemoglobin or red blood cell function, impairs systemic oxygen delivery and affects approximately one-fourth of the global population, particularly pregnant women and young children (Probst et al., 2022). Its causes are multifactorial, including iron deficiency, chronic disease, and environmental influences. During pregnancy and early childhood—periods of elevated iron demand—the condition carries significant risks. Iron-deficiency anemia in pregnancy is associated with miscarriage, premature delivery, low birth weight, and maternal mortality due to compromised fetal oxygenation and intrauterine growth restriction (Javed et al., 2020). In children, anemia impairs cognitive and motor development and academic performance, with prevalence reaching up to 20% even in high-income countries such as the United States (Knez & Liang, 2024).

4.2. Common Causes of Anemia in Rural Areas

Anemia remains a major public health concern in rural areas, driven primarily by nutritional deficiencies and socio-economic constraints. Iron deficiency accounts for approximately half of global cases and is highly prevalent in low- and middle-income countries such as India and Indonesia, particularly among adolescent girls and women with inadequate dietary intake (Kaviya & Dhanushya, 2024; Sari et al., 2022). In Nigeria, childhood anemia is strongly associated with chronic malnutrition and poor anthropometric status (Moyegbone et al., 2024).

Chronic disease and inflammation further contribute, as shown in rural Ethiopia where maternal anemia was linked to both inflammatory conditions and nutrient deficits (Gebreegziabher & Stoecker, 2017; chaparro & Suchdev, 2019). These factors, compounded by poverty and limited healthcare access, necessitate integrated clinical and public health interventions.

4.3. Challenges in Traditional Hemoglobin Screening

Conventional hemoglobin screening methods, including complete blood count (CBC) testing and point-of-care hemoglobinometers, require invasive blood sampling and laboratory support. Although accurate, these methods are logistically challenging in rural and resource-limited settings, where venipuncture demands sterile conditions, trained personnel, and proper waste disposal (Kim et al., 2020). Portable devices such as HemoCue improve accessibility but still require reagents, calibration, and controlled environments, with accuracy affected by temperature and humidity fluctuations (Mukhopadhyay et al., 2018).

Needle-related anxiety reduces screening compliance, particularly among children and older adults (Bardale et al., 2023). Recurring consumable costs and infrastructure requirements further limit large-scale and mobile implementation (Bhargava et al., 2022; Sahu et al., 2023).

4.4. Photoplethysmography (PPG) in Hemoglobin Estimation

Photoplethysmography (PPG) is a non-invasive optical technique that detects microvascular blood volume changes using red and infrared light absorption. Although widely used for heart rate and oxygen saturation monitoring, recent studies demonstrate its potential for hemoglobin estimation. Ghazanfari et al. (2021) reported machine learning–based PPG models achieving a mean absolute error below 1.2 g/dL, clinically acceptable for screening. Raj et al. (2022) further showed high sensitivity and specificity using regression-based approaches.

Limitations include susceptibility to motion artifacts, low perfusion, ambient light interference, and individual variations such as skin pigmentation and temperature. Nevertheless, PPG remains a cost-effective and scalable option for non-invasive hemoglobin screening in resource-limited settings.

4.5. Heart Rate and SpO_2 Monitoring Using PPG

Photoplethysmography (PPG) is a non-invasive optical method used to measure heart rate (HR) and oxygen saturation (SpO_2) via red and infrared light absorption. Its accuracy under resting conditions is well established (Allen, 2016). PPG-based pulse oximeters reliably estimate SpO_2 by distinguishing oxygenated and deoxygenated hemoglobin absorption characteristics (Elgendi et al., 2019), and wearable systems support continuous monitoring, particularly in geriatric populations at risk of arrhythmia and hypoxemia (Tamura et al., 2017).

Signal integrity may be affected by motion artifacts, ambient light, and physiological variability; however, adaptive filtering techniques significantly improve measurement accuracy under motion conditions (Nemcova et al., 2020).

4.6. Non-Invasive Hemoglobin Estimation

Non-invasive hemoglobin estimation provides an alternative to conventional blood-based testing, particularly in resource-limited settings. Techniques including photoplethysmography (PPG), near-infrared spectroscopy (NIRS), and pulse CO-oximetry estimate hemoglobin through tissue light absorption analysis. Ghazanfari et al. (2021) demonstrated reliable PPG-based hemoglobin prediction using machine learning models, while Zhang et al. (2021) showed that multispectral PPG improves accuracy across varying skin pigmentation and perfusion conditions.

Advances integrating AI-driven pattern recognition and signal correction continue to enhance performance, expanding applications in emergency care, maternal health, and large-scale screening (Raj et al., 2022), positioning non-invasive hemoglobin monitoring as a scalable point-of-care solution.

4.7. Hemoglobin, Heart Rate, and SpO_2 in Anemia

The relationship among hemoglobin (Hb), heart rate (HR), and oxygen saturation (SpO_2) is central to anemia evaluation. Reduced Hb limits oxygen delivery, prompting compensatory increases in cardiac output through elevated HR (Weiskopf et al., 2021), which may precede clinical symptoms.

SpO_2 often remains normal in mild to moderate anemia because pulse oximeters measure saturation percentage rather than absolute Hb concentration (Luks & Swenson, 2020). Consequently, normal SpO_2 does not rule out impaired oxygen transport. Simultaneous assessment of Hb, HR, and SpO_2 such as low Hb with elevated HR and normal SpO_2 provides a more accurate indication of compensated anemia and supports earlier detection.

4.8. Mobile App Interface and Usability in Health Monitoring

Mobile health applications are reshaping healthcare delivery; however, their efficacy is limited by challenges related to usability and user satisfaction. A mixed-methods investigation conducted in Bangladesh, which assessed 36 health applications, revealed that 61% of the identified usability issues were classified as either catastrophic or major. This, in turn, resulted in significantly reduced System Usability Scale (SUS) scores and hindered user adoption (Islam et al., 2020). Moreover, Mena and colleagues (2020) found a positive correlation between user interface design—particularly the use of large icons and visually appealing components—and increased satisfaction and accuracy in vital sign monitoring among the elderly.

Usability further encompasses user engagement and the facilitation of regular application use. Personalization, goal-setting features, and interactive components demonstrably affect sustained application utilization, as evidenced by applications created for chronic disease management (Shah et al., 2023). Technical impediments, encompassing language barriers, digital literacy deficits, internet connectivity limitations, and smartphone proficiency, were also recognized as significant constraints, especially within rural contexts (Shah et al., 2023).

4.9. WiFi and IoT Integration in Health Monitoring Systems

Recent advances in WiFi-enabled microcontrollers, particularly the ESP32, enable real-time transmission of wearable health data to cloud platforms. Ferdous et al. (2023) implemented an ESP32-based system integrating pulse rate, temperature, and SpO_2 sensors with WiFi data transmission for remote monitoring and alerts. Similarly, Ibañez-Castillo (2024) developed an ESP32 IoT wearable incorporating ECG, SpO_2, and temperature sensors, demonstrating reliable WiFi communication and accurate health trend tracking. These studies highlight ESP32-based frameworks as scalable solutions for multi-sensor, real-time health monitoring.

However, WiFi integration increases power consumption despite offering ~100 m range and high bandwidth (Cheng & Gupta, 2022). To address this, Huang et al. (2024) implemented adaptive frequency hopping and optimized ESP32-WROOM communication for stable physiological and location data transmission.

4.10. Health Mapping

Digital health geographic information systems (GIS) support real-time tracking and visualization of health data for disease surveillance and service planning. During COVID-19, mobile GIS tools mapped high-infection areas to guide interventions (Kamel Boulos & Geraghty, 2020). In resource-limited settings, GPS-enabled applications improve geo-tagged surveillance and targeted care delivery (Kostkova et al., 2016).

AI and cloud integration enhance predictive modeling and data accuracy (Huang et al., 2022). Beyond outbreak response, GIS platforms assess chronic disease trends, maternal healthcare access, and regional anemia disparities (Abdulkader et al., 2023), while optimizing mobile clinic deployment in underserved communities (Ali et al., 2019).

4.11. Related Studies

The utilization of non-invasive photoplethysmography (PPG) for hemoglobin assessment has garnered considerable attention in global research endeavors, with the objective of enhancing the availability of health diagnostics.

In the investigation entitled "A Non-Invasive Hemoglobin Detection Device Based on Multispectral PPG," investigators engineered a wearable system employing multiple LED wavelengths and incorporated machine learning models, including AdaBoost and neural networks.

A comparable methodology was adopted in the research "Non-invasive Measurement of Hemoglobin for Rural India using Artificial Intelligence," wherein researchers devised a multi-wavelength PPG device, integrated with machine learning regression, to facilitate non-invasive hemoglobin level estimation Using five LED wavelengths and an OPT101 photodiode, the system showed an average error of only 0.36 dL compared to invasive methods. Moreover, the device allowed for continuous monitoring of SpO_2 and blood pressure. This made it suitable for use in rural healthcare settings, thanks to its portability, cost-effectiveness, and environmentally friendly design (Mude, 2022).

In a veterinary surgical context, the study "Feasibility and Accuracy of Noninvasive Continuous Hemoglobin Monitoring Using Transesophageal PPG" provided additional support, showing a strong correlation ($r \approx 0.79$) between hemoglobin levels estimated using transesophageal PPG in pigs and direct blood gas measurements. This indicated promising results for non-invasive, intraoperative Hb tracking (Pintavirooj et al., 2021).

The investigation titled "Real-Time Analysis of PPG Signal for SpO_2 and Pulse Rate Measurement" further explored the domain of real-time physiological monitoring. This research endeavor culminated in the development of an economical, portable pulse oximeter, which utilized red and infrared LEDs in conjunction with a photodiode for PPG signal acquisition. The processing of the PPG signals' AC and DC components was executed via LabView software, which incorporated low-pass and moving average filters to diminish noise and motion artifacts. SpO_2 levels were determined through the application of a normalized red-to-infrared absorption ratio, while pulse rate was established through time-domain peak detection.

The study's results demonstrated consistent accuracy when contrasted with established pulse oximeters, thereby confirming the system's applicability for real-time monitoring in critical care settings (Bagha et al., 2021).

Moreover, the research, "Noninvasive Portable Hemoglobin Concentration Monitoring System Using the MAX30102 Sensor," introduced an affordable, infrared and red LED-based clip sensor. This sensor achieved a 90.9% accuracy rate when compared to the cyanmethemoglobin method. As a result, this simple yet effective design offered an accessible solution for point-of-care screening, particularly in resource-constrained regions (Tan et al., 2025).

3. METHODOLOGY

3.1. Research Design

This study employed a Research and Development (R&D) approach to design, develop, and evaluate the PULSE device. The portable, non-invasive system uses a MAX30102 PPG sensor integrated with an ESP32, OLED display, Wi-Fi, GPS, and a web platform to monitor hemoglobin (Hb), SpO_2, heart rate (HR), systolic (SBP), and diastolic blood pressure (DBP) in real time. The process included needs assessment, material selection, circuit integration, firmware programming in Arduino IDE for signal processing, website development, prototype fabrication, calibration with clinical references, and usability testing.

3.2. Sampling and Participants

A Purposive sampling recruited 50 participants with expertise in community and clinical health monitoring: 15 health professionals, 20 barangay health workers, and 15 LGU staff/administrators. Their rural healthcare experience supported evaluation of the PULSE system's usability, accuracy, and functionality.

An additional 30 individuals who had completed laboratory assessments participated in validation, enabling comparison of PULSE measurements of hemoglobin (Hb), blood pressure (BP), heart rate (HR), and oxygen saturation (SpO_2) with clinical reference standards. Ethical protocols, including informed consent and confidentiality, were strictly maintained.

3.3. Material Selection and Procurement

Table 1. Research Materials

MATERIALS	PICTURE	UNIT	QTY	PURPOSE
A9G Module GSM/GPRS+GPS		piece	1	This module adds onboard geolocation tagging to collected health data.
ESP32 Microcontroller		piece	1	Acts as the main processor of the main device, handling sensor data, vital sign estimation, and Wi-Fi transmission.
ESP32 Mini Microcontroller		piece	1	The SMS device's primary processor handles everything: it manages sensor data, processes that information, and then sends messages using GSM technology.
Filament		piece(s)	2	Used in 3D printing to create the device casing, providing durability, portability, and protection for internal electronics.
Header Pin		piece(s)	2	Acts as a connector between modules and the PCB, allowing easy attachment, testing, and replacement without permanent soldering.
LED		pieces(s)	2	Indicates when the system is powered and ready for use.

Lithium-Ion Battery (7.4V 2200mAh)		piece(s)	2	Stores energy to power the device when solar input is not available; ensures continuous operation.
MAX30102 PPG Sensor		piece	1	Measures heart rate and oxygen saturation (SpO_2) using red and infrared light; provides the PPG signal used for estimating hemoglobin levels and blood pressure.
OLED Display		piece	1	Visually displays the real-time readings of Hemoglobin (Hb), SpO_2, Heart Rate (HR), and Blood Pressure (BP) to the user.
Printed Circuit Board	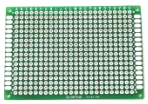	piece	1	Provides a stable platform for mounting and interconnecting components, ensuring compact design, fewer wiring errors, and reliable signal transmission.
Sim Card		piece(s)	2	Acts as a connector between modules and the PCB, allowing easy attachment, testing, and replacement without permanent soldering.
Switch		piece	1	A SIM card in the A9G GSM/GPRS+GPS module enables mobile connectivity, allowing real-time transmission of location and health data. It ensures reliable monitoring and GPS-based logging even without Wi-Fi.
TP4056 - TC4056A Lithium Battery Charger and Protection Module		piece(s)	2	Manages lithium-ion battery charging with built-in protection against overcharge, discharge, and short circuits, ensuring safe and stable power supply.
Wires		set	1	Used to establish electrical connections between the components of the device, such as linking the PPG sensor (MAX30102) display module,

microcontroller (ESP32), power source, and other modules.

3.4. System Architecture Design

Figure 1. Actual Prototype

3.5. Circuit Integration

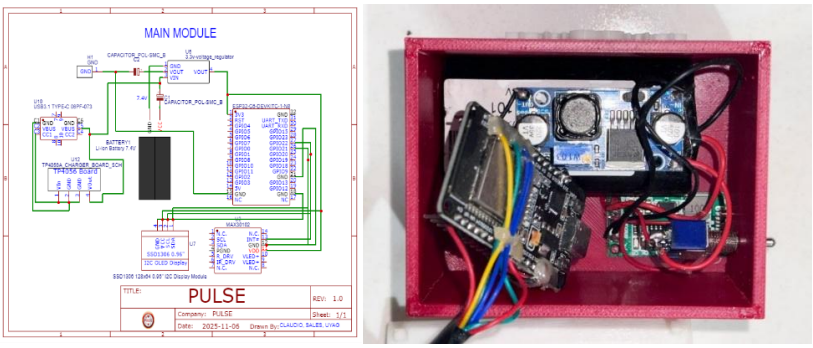

Figure 2. *Circuit of the Main Device*

The circuit diagram depicts the comprehensive electrical architecture of the PULSE main device. This configuration incorporates the ESP32 microcontroller, the MAX30102 photoplethysmography (PPG) sensor, an OLED display, a lithium-ion battery (7.4V 2200mAh), a TP4056–TC4056A lithium battery charger and protection module, and a power switch. Consequently, the design facilitates the acquisition of PPG signals, the processing of these data for hemoglobin estimation, and the real-time display of the results, all while ensuring effective power management.

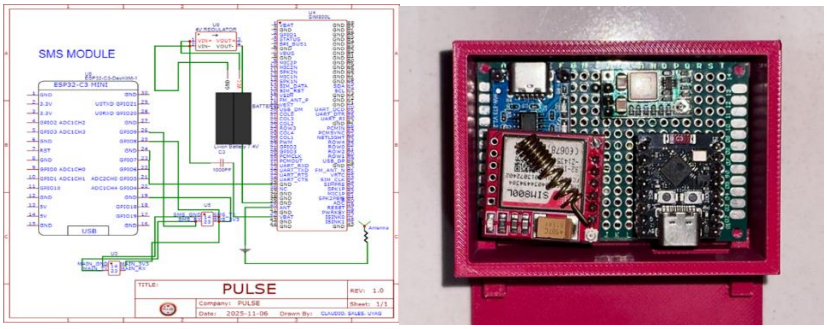

Figure 3. *Circuit of the SMS Device*

The circuit diagram shows how the PULSE SMS device is set up. This device is designed to send alerts and hemoglobin readings using GSM technology. The assembly incorporates the ESP32 Mini microcontroller, an A9G GSM/GPRS+GPS module, a SIM card interface, and the TP4056–TC4056A lithium battery charger and protection module. These connections facilitate the wireless sending of messages and GPS capabilities, all while keeping things portable and conserving energy.

3.4. Firmware Programming

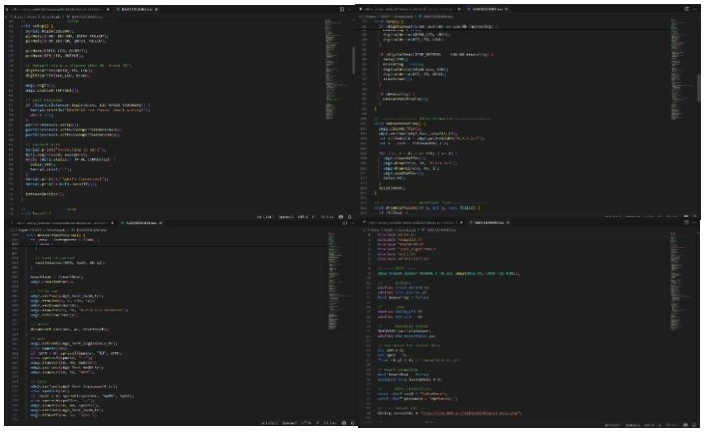

Figure 4. *Hardware Programming Code*

The PULSE system was developed using the Arduino IDE with modular C/C++ architecture to support sensor acquisition, signal processing, computation, and wireless communication. Upon startup, the microcontroller initializes the PPG sensor, OLED display, Wi-Fi, and GPS modules, then continuously processes signals using smoothing, peak detection, and noise reduction algorithms to enhance measurement reliability.

Embedded Multiple Linear Regression (MLR) models analyze extracted PPG features to estimate hemoglobin concentration, systolic and diastolic blood pressure, oxygen saturation, and heart rate in real time. Timing control and buffering mechanisms ensure stable sampling and synchronized parameter computation.

Processed data are displayed locally on the OLED interface and transmitted via Wi-Fi to a web-based platform for remote logging and visualization, with GPS-tagged records enabling geospatial health monitoring. Built-in error-handling routines maintain operational stability during sensor interruption, communication latency, and power variability.

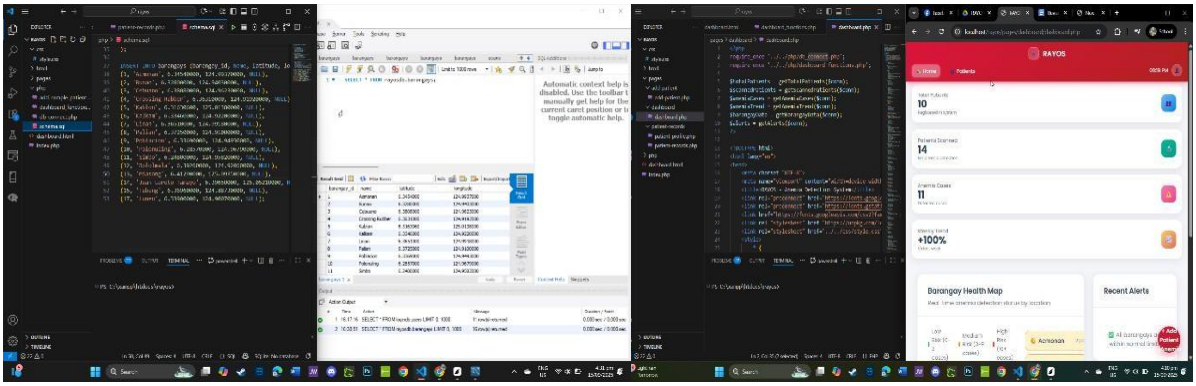

Figure 5. *Website Programming Code*

The IoT-driven PULSE system follows a client-server architecture integrating embedded hardware, backend processing, and web-based visualization. Sensor-equipped microcontrollers programmed in C++ transmit physiological data via HTTP to a PHP backend, where it is validated and

stored in a MySQL database containing patient, device, and measurement records. The frontend, built with HTML, CSS, and JavaScript, asynchronously retrieves data for real-time visualization and geospatial mapping using JavaScript mapping libraries, enabling centralized and scalable health monitoring.

3.3. Initial Testing

To obtain relevant and accurate data for each research question, the following data gathering procedures were conducted:

3.3.1. Hemoglobin Estimation Using PPG-Derived Parameters

Data were be gathered by conducting multiple test scans using the MAX30102 infrared Photoplethysmography (PPG) sensor on individuals with clinically verified hemoglobin levels, confirmed through Complete Blood Count (CBC) tests at the Rural Health Unit in Tupi, South Cotabato.

The following PPG signal features were extracted from each scan:

a. **Pulse Width (W):** Duration of one pulse waveform cycle

b. **Peak Interval (T):** Time between consecutive peaks, inversely related to heart rate

c. **Root Mean Square (RMS):** Signal power linked to hemoglobin density

These features were applied to a multivariable linear regression model to estimate hemoglobin levels:

$$Hb_{estimated} = \beta_0 + \beta_1 W + \beta_3 T + \beta_3 RMS$$

3.3.2. Blood Pressure Measurement and Feature Extraction

To integrate hypertension screening, systolic and diastolic blood pressure readings were collected using a clinically validated automatic sphygmomanometer as the reference.

The data were gathered by conducting multiple test scans using the MAX30102 infrared Photoplethysmography (PPG) sensor on individuals whose blood pressure readings had been clinically verified through sphygmomanometer measurements at the Rural Health Unit in Tupi, South Cotabato.

From each PPG waveform, the following signal features were extracted:

i. **Pulse Width (W):** Duration of one pulse cycle, corresponding to the time between signal rise and fall.

ii. **Perfusion Index (PI):** Ratio of pulsatile to non-pulsatile signal components, indicating arterial blood flow strength.

iii. **Root Mean Square (RMS):** Statistical measure of signal power, representing waveform amplitude and arterial compliance.

These features will then be applied to a multivariable linear regression (MLR) model to estimate systolic blood pressure (SBP), expressed in millimeters of mercury (mmHg), as follows:

$$SBP_{estimated} = \beta_0 + +\beta_1 W + \beta_2 PI + \beta_3 RMS$$

Similarly, diastolic blood pressure (DBP) data were obtained from multiple PPG scans that were conducted on participants with clinically measured BP values at the Rural Health Unit in Tupi, South Cotabato.

From each PPG waveform, the following signal features were extracted:

1. **Pulse Width (W):** Duration of one pulse cycle, corresponding to the time between signal rise and fall.

2. **Perfusion Index (PI):** Ratio of pulsatile to non-pulsatile signal components, indicating arterial blood flow strength.

3. **Root Mean Square (RMS):** Statistical measure of signal power, representing waveform amplitude and arterial compliance.

These features were then utilized in a multivariable linear regression (MLR) model to estimate diastolic blood pressure (DBP), expressed in millimeters of mercury (mmHg), as follows:

$$DBP_{estimated} = \beta_0 + +\beta_1 W + \beta_2 PI + \beta_3 RMS$$

3.3.3. Heart Rate and SpO_2 Estimation Using MAX30102 Sensor

The MAX30102 sensor simultaneously measured red light (660 nm) and infrared (IR, 880–940 nm) absorption through photoplethysmography (PPG). These dual wavelengths will enable the estimation of both heart rate (HR) and oxygen saturation (SpO_2) using the following algorithms:

a. Heart Rate Estimation

Method:

1. Extract the IR PPG signal

2. Apply a Bandpass Filter (0.5–4 Hz) to isolate pulse frequency

3. Detect peaks of the waveform to calculate inter-beat intervals (IBI)

Formula:

$$HR\ (bpm) = \frac{60}{Average\ IBI\ (seconds)}$$

b. SpO_2 Estimation

SpO_2 was estimated from the relative absorption of red and IR light, based on the principle that oxygenated and deoxygenated hemoglobin absorbed light differently.

Compute AC/DC ratio for both red and IR signals:

$$R = \frac{\left(\frac{AC_{red}}{DC_{red}}\right)}{\left(\frac{AC_{IR}}{DC_{IR}}\right)}$$

1. Apply an empirical regression formula:

$$SpO^2 = 110 - 25 \times R$$

3.3.4. System vs. Clinical Device Comparison

Data were collected from 10 participants, with each participant undergoing 3 repeated trials. Hemoglobin levels were measured in a laboratory setting using both a hematology analyzer (machine) and manual CBC testing as reference standards, alongside parallel measurements using the PULSE system. For SpO_2 and heart rate, measurements were obtained from a clinically validated pulse oximeter across 10 trials per participant and were compared with simultaneous readings from the PULSE device. To verify the accuracy of blood pressure readings, measurements from 10 participants were also taken using a standard sphygmomanometer and were compared with corresponding readings from the PULSE system.

This resulted in paired datasets for each parameter: hemoglobin, SpO_2, heart rate, and blood pressure across machine/manual reference methods and PULSE trials. The collected data were then analyzed to compute mean values, accuracy rates, mean differences, and correlation coefficients, allowing for a robust evaluation of the measurement validity and reliability of the PULSE system.

3.3.5. Real-Time Data Display

For each health scan, the time interval was recorded using a timer and the device logs, starting from the completion of the sensor reading up to two points of output:

a. the display of results on the built-in OLED screen of the device, and

b. the arrival of data on the website via Wi-Fi transmission.

A total of 30 dependent trials were conducted for both outputs to determine the average response time and to compare whether one method delivered results significantly faster than the other.

3.3.6. Data Logging and Health Mapping

The website will be tested under both stable and unstable Wi-Fi conditions to examine its reliability in real-world settings. The website-generated logs, which included timestamps, GPS coordinates, and physiological readings (Hb, HR, SpO_2, and BP), were compared with manually recorded data to check for consistency and accuracy. The mapping feature of the website was also tested during live scans to ensure that data points were plotted correctly and in real time. A total of 30 trials per connectivity condition were conducted to validate the accuracy of the logging and mapping functions.

3.3.7. *System Unit Testing and User Evaluation*

Unit testing was conducted to evaluate the PULSE system's performance, ensuring that each component particularly the MAX30102 sensor, GPS module, OLED display, and website met the standards of accuracy, functionality, and acceptability:

a. Accuracy was assessed by verifying whether the MAX30102 sensor module could correctly measure hemoglobin levels, oxygen saturation (SpO_2), heart rate, and blood pressure, and whether the website could classify these readings based on the trained classification model.

b. Functionality was tested by evaluating if all integrated modules such as the sensor readings, real-time OLED display, and website communication worked reliably and consistently under

different testing conditions. This included verifying website-based data logging and location-based health mapping features.

c. Acceptability was evaluated by gathering user assessments on whether the system's physical design, and mobile interface were intuitive, usable, and non-intimidating, particularly for health workers in rural or underserved communities.

The study adopted a Research and Development (R&D) approach to evaluate the performance and reliability of the PULSE system. Testing sessions simulated various physiological scenarios to analyze system response. Sensor accuracy was compared against clinically validated standard devices, while the website's capability to process, log, and classify user data was critically examined. Emphasis was placed on real-time performance, and the stability of Wi-Fi communication between hardware and the website.

3.3. Data Analysis

To evaluate the performance, accuracy, and usability of the PULSE (Predictive Utility for Learning Systems in Evaluating Anemia and Hypertension), both descriptive and inferential statistical techniques will be applied to the collected data:

3.3.1. Accuracy of the MLR Model for Hemoglobin and Blood Pressure Prediction

The PULSE Multiple Linear Regression (MLR) models for predicting hemoglobin (Hb), Systolic blood pressure (SBP), and Diastolic blood pressure (DBP) from PPG features will be validated against Complete Blood Count (CBC) and sphygmomanometer measurements. Three trials per participant will be averaged to reduce random error.

Performance will be evaluated using R^2, Root Mean Square Error (RMSE), Mean Absolute Error (MAE), and Mean Absolute Percentage Error (MAPE). Pearson correlation and Bland–Altman analysis will assess association and agreement. High R^2, low error values, and minimal bias will indicate accurate and reliable non-invasive estimation.

3.3.2. Accuracy of Physiological Measurements

The accuracy of PULSE measurements for hemoglobin (Hb), oxygen saturation (SpO_2), heart rate (HR), blood pressure (BP) will be compared with clinically accepted standards. First, the mean of three trial values (T1–T3) per participant will be computed to reduce random error. Next, a one-way repeated measures ANOVA will be used to test whether there will be significant differences across the three methods (Machine, Manual, and PULSE) while accounting for within-participant variability. Pairwise comparisons will further be conducted using paired t-tests to identify systematic differences between methods.

To assess reliability and consistency, the Intraclass Correlation Coefficient (ICC, two-way random effects, absolute agreement) will be computed across the three methods. Agreement between PULSE and the pulse oximeter will further be examined using Bland–Altman analysis, which will quantify mean bias and 95% limits of agreement. Finally, Pearson correlation coefficients will be calculated to determine the strength and direction of the linear relationship between the measurement methods.

3.3.3. Comparison of Blood Pressure (BP) Measurements Between the Sphygmomanometer and the PULSE System

To determine whether there is a significant difference between blood pressure (BP) measurements obtained using a standard sphygmomanometer and those estimated by the PULSE system, a paired t-test was conducted for both systolic blood pressure (SBP) and diastolic blood

pressure (DBP) values. This statistical test evaluates whether the mean BP readings from both methods differ significantly, considering measurement variability and consistency across participants.

3.3.4. Mean Response Time of the PULSE System

The system's efficiency in displaying results will be assessed by measuring response times between Wi-Fi transmission to the website and OLED on-device display. Paired t-tests will be used to compare these two methods across 30 paired trials. Descriptive statistics (mean and standard deviation of differences), effect size (paired Cohen's d), and 95% confidence intervals will also be computed to evaluate whether observed differences will be statistically significant and practically meaningful.

3.3.5. System Accuracy, Functionality, and Acceptability

Table 2. Likert Scale for Evaluation Scores

Code	*Mean Range*	*Description*
5	*4.20-5.00*	*Strongly Agree*
4	*3.40-4.19*	*Agree*
3	*2.60-3.39*	*Moderately Agree*
2	*1.80-2.59*	*Disagree*
1	*1.00-1.79*	*Strongly Disagree*

Note: Adapted from Morillo, J. P., Cruz, C. E., & Angeles, J. M. (2021).

System evaluation will also consider user experience and performance feedback. A 5-point Likert scale checklist will be administered to 50 participants to assess accuracy, functionality, and acceptability across sensing, display, website logging, and classification modules. Mean scores will be interpreted using standard ranges (Strongly Disagree to Strongly Agree), providing both descriptive and inferential evidence of system usability.

3.3.6. Trained Classification Model

Once the four vital parameters: Hemoglobin (Hb), Heart Rate (HR), Blood Oxygen Saturation (SpO_2), and Blood Pressure (SBP and DBP) were estimated, the system forwarded the results to a trained classification logic model. This model interpreted the combined readings using clinically supported reference patterns for anemia and hypertension detection.

The classification logic operated through if–else conditional rules and regression-based thresholds, derived from established medical guidelines and literature. This enabled the PULSE system to categorize the user's physiological status as normal or at risk of anemia and/or hypertension. The interpretations were informed by the reference tables below:

Table 3. Interpretation of Hb, SpO_2, and HR Readings for Anemia Detection

Hb Level	**SpO_2**	**Heart Rate (HR)**	**Interpretation**
Low	Normal (≥95%)	Elevated (>100 bpm)	Compensated anemia: early-stage anemia where elevated HR compensates for low Hb
Low	Low (<94%)	Normal or Elevated	Advanced anemia or concurrent hypoxemia;

			possible respiratory comorbidity
Normal	Normal	Normal	No anemia or healthy physiological status
Low	Normal	Normal	Mild or early anemia with no hemodynamic compensation yet

Note: Adapted from Hasan et al. (2018), Wang et al. (2017), Zhu et al. (2021), Chen et al. (2022), Bai et al. (2016), and Kwon & Kim (2022)

Table 4. Interpretation of SBP and DBP Readings for Hypertension Detection

Systolic BP (SBP)	Diastolic BP (DBP)	Interpretation	Physiological Implication
<120 mmHg	<80 mmHg	Normal Blood Pressure	Indicates healthy cardiovascular regulation and normal arterial elasticity.
120–129 mmHg	< 80 mmHg	Elevated Blood Pressure	Early vascular resistance; may progress to hypertension if lifestyle risks persist.
130–139 mmHg	80–89 mmHg	Stage 1 Hypertension	Mild elevation; often asymptomatic but suggests early arterial stiffness or increased cardiac workload.
≥140 mmHg	≥90 mmHg	Stage 2 Hypertension	Significant increase in vascular resistance; requires medical evaluation and monitoring.

Note: Classification adapted from World Health Organization (WHO, 2023) and American Heart Association (AHA, 2023) guidelines for hypertension management.

Table 5. Interpretation of Hb and BP Status

Hb Status	BP Status	Interpretation	Recommendation
Normal	Normal	Healthy cardiovascular and hematologic profile.	Maintain balanced lifestyle and routine monthly monitoring.
Low	Normal	Anemia without hypertension.	Focus on iron-rich diet and hydration; monitor BP regularly.
Normal	Elevated/Stage 1 Hypertension	Isolated hypertension.	Reduce salt intake, manage stress, and maintain daily activity.
Low	Elevated/Stage 1 Hypertension	Possible Compensatory Hypertension. The body may increase cardiac output to compensate for anemia.	Address anemia first (diet, iron supplementation) while monitoring BP weekly.
Low	Stage 2 Hypertension or Higher	High-risk comorbidity: potential cardiovascular strain and reduced oxygen delivery.	Immediate medical evaluation recommended; bring PULSE data to a clinic or hospital.
Very Low Hb	Any Hypertension	Critical condition: may indicate chronic disease (e.g., renal or cardiac origin).	Seek urgent professional medical assessment.

Note: Adapted from Gupta et al. (2019), Kario (2018), World Health Organization (2023), and Whelton et al. (2023).

4. FINDINGS

This presents the comprehensive findings of the study on PULSE (Predictive Utility for Learning Systems in Evaluating Anemia and Hypertension), focusing on accuracy, reliability, system performance, and functionality. Findings were derived from calibration and validation tests comparing PULSE outputs with standard clinical instruments, including hematology analyzers, manual complete blood count (CBC) tests, sphygmomanometers, and pulse oximeters. Statistical analyses were conducted to assess agreement, error margins, correlation strength, and operational efficiency.

The data were gathered by conducting multiple test scans using the MAX30102 infrared Photoplethysmography (PPG) sensor on individuals' data whose hemoglobin levels had been clinically verified through Complete Blood Count (CBC) tests at the Rural Health Unit in Tupi, South Cotabato.

From each PPG waveform, the following signal features were extracted:

1. Pulse Width (W): Duration of one pulse cycle.
2. Peak Interval (T): Time between consecutive peaks, inversely proportional to heart rate.
3. Root Mean Square (RMS): Signal power, reflecting hemoglobin density.

These features were then applied to a multivariable linear regression (MLR) model to estimate hemoglobin levels, expressed in g/L, as follows:

$$Hb_{estimated} = \beta_0 + +\beta_1 \boldsymbol{W} + \beta_2 \boldsymbol{T} + \beta_3 \boldsymbol{RM}$$

The regression coefficients were obtained during model training, resulting in the following MLR equation:

$$Hb_{estimated} = 173.576229 - 78.82609\ W - 54.976575\ T + 0.157445\ RMS$$

This regression equation demonstrates how specific PPG-derived features contribute to estimating hemoglobin concentration in a non-invasive manner.

Table 6. Accuracy Metrics for of the MLR Model for Predicting Hemoglobin Levels

MLR Model	R-squared	RMSE	Mean Absolute Error	MAPE
	$= \frac{SSR}{SST}$	$= \sqrt{\sum_{i=1}^{n} \frac{(y-y_1)^2}{n}}$	$= \frac{1}{n}\sum_{i=1}^{n} \lvert yi - \hat{y}_i \rvert$	$= \frac{1}{n}\sum_{i=1}^{n} 1 \frac{A_i - F_i}{A_i}$
Model	0.99	1.1797	0.9593	0.80%

Table 6 presents the accuracy metrics of the Multivariable Linear Regression (MLR) model used to predict hemoglobin levels from PPG-derived features. The model achieved an R-squared value of 0.99, indicating that 99% of the variance in hemoglobin levels was explained by the predictors. The Root Mean Square Error (RMSE) of 1.1797 g/L and Mean Absolute Error (MAE) of 0.9593 g/L reflect minimal deviations between predicted and actual values. Furthermore, the Mean Absolute Percentage Error (MAPE) of 0.80% demonstrates the high precision of the model. These metrics collectively confirm that the MLR model provides reliable and accurate estimations of hemoglobin levels, making it suitable for non-invasive anemia screening applications.

Table 7. Comparison of Predicted and Actual Hemoglobin Levels Using PULSE

Patient	Predicted	Actual	Error	|Error|	% Error
1	124.36	125	-0.64	0.64	0.51%
2	116.03	118	-1.97	1.97	1.67%
3	135.544	134	1.54	1.54	1.15%
4	102.96	102	0.96	0.96	0.94%
5	145.61	146	-0.39	0.39	0.27%
6	131.29	130	1.29	1.29	0.99%
7	111.77	113	-1.23	1.23	1.09%
8	149.86	149	0.86	0.86	0.58%
9	107.52	108	-0.48	0.48	0.44%
10	138.21	138	0.21	0.21	0.15%
11	123.26	124	-0.74	0.74	0.60%
12	116.1	117	-0.9	0.9	0.77%
13	133.1	132	1.1	1.1	0.83%
14	102.1	101	1.1	1.1	1.09%
15	146.16	147	-0.84	0.84	0.57%
16	129.09	129	0.09	0.09	0.07%
17	113.59	115	-1.41	1.41	1.23%
18	151.2	151	0.2	0.2	0.13%
19	107.29	106	1.29	1.29	1.22%
20	136.87	136	0.87	0.87	0.64%
21	123.34	126	-2.66	2.66	2.11%
22	117.91	119	-1.09	1.09	0.92%
23	135.85	135	0.85	0.85	0.63%
24	103.2	100	3.2	3.2	3.20%
25	147.42	148	-0.58	0.58	0.39%
26	130.26	131	-0.74	0.74	0.56%
27	113.27	114	-0.73	0.73	0.64%
28	150.33	150	0.33	0.33	0.22%
29	109.18	109	0.18	0.18	0.17%
30	139.31	139	0.31	0.31	0.22%

Table 7 presents the comparison between the predicted and actual hemoglobin (Hb) values across 30 patient samples. The table includes the computed error, absolute error, and percentage error for each prediction. Results show that most predictions fall within a low error margin, indicating that the MLR model achieves high accuracy in estimating Hb levels. Only a few samples exceeded a 2% error, while the majority remain below 1%, demonstrating the model's reliability and strong agreement with the actual laboratory values.

Table 8. Mean Hemoglobin Measurements Using Machine, Manual, and PULSE Methods

PARTICIPANT	MACHINE (g/L)			MANUAL (g/L)			PULSE (g/L)		
	T1	T2	T3	T1	T2	T3	T1	T2	T3
P1	133	129	129	127	127	127	130	128	129
P2	139	138	136	130	133	133	135	134	136
P3	115	117	120	117	113	113	116	115	117
P4	139	138	137	130	133	130	135	134	133
P5	126	127	128	123	123	123	125	124	126
P6	132	131	131	140	137	140	134	133	135
P7	160	161	161	163	163	167	162	163	165
P8	134	131	134	137	137	137	135	134	136
P9	174	177	175	170	170	167	172	171	170
P10	162	162	162	167	167	167	164	163	165
Mean	141.4	141.1	141.3	140.4	140.3	140.4	140.8	139.9	141.2

Table 8 shows that hemoglobin measurements from Machine, Manual, and PULSE methods were closely aligned, with overall means of 141.3 g/L, 140.4 g/L, and 140.6 g/L, respectively. The minimal differences across trials and methods indicate that PULSE provides consistent and reliable readings comparable to standard clinical measurements.

Table 9. One-Way ANOVA Summary for Hemoglobin Measurements Across Methods

Source of Variation	*SS*	*df*	*MS*	*F*	*P-value*	*F crit*
Between Groups	*24.44444*	*8*	*3.055556*	*0.009508*	*1*	*2.042986*
Within Groups	*28924.4*	*90*	*321.3822*			
Total	*28948.84*	*98*				

Table 9 shows the ANOVA results with a p-value of 1.000, which is much higher than the 0.05 significance level. This indicates that the null hypotheses cannot be rejected, meaning there is no significant difference between the hemoglobin levels measured by the Machine, Manual, and PULSE methods. Thus, PULSE demonstrates comparable accuracy with both clinical and manual standards, supporting the overall hypothesis that it can reliably measure hemoglobin, SpO_2, and heart rate within clinically accepted ranges.

The data were gathered by conducting multiple test scans using the MAX30102 infrared Photoplethysmography (PPG) sensor on individuals whose blood pressure readings were clinically verified through sphygmomanometer measurements at the Rural Health Unit in Tupi, South Cotabato.

From each PPG waveform, the following signal features were extracted:

1. Pulse Width (W): Duration of one pulse cycle, corresponding to the time between signal rise and fall.

2. Perfusion Index (PI): Ratio of pulsatile to non-pulsatile signal components, indicating arterial blood flow strength.

3. Root Mean Square (RMS): Statistical measure of signal power, representing waveform amplitude and arterial compliance.

These features were then applied to a multivariable linear regression (MLR) model to estimate systolic blood pressure (SBP), expressed in millimeters of mercury (mmHg), as follows:

$$SBP_{estimated} = \beta_0 + +\beta_1 \boldsymbol{W} + \beta_2 \boldsymbol{PI} + \beta_3 \boldsymbol{RMS}$$

Where the coefficients were determined from model training:

$$SBP_{estimated} = 99.704 + 0.1416W - 0.0684PI + 16.2705RMS$$

This regression model demonstrates how specific PPG-derived features are mathematically correlated with arterial systolic pressure, enabling non-invasive estimation of SBP through optical sensing.

Table 10. Accuracy Metrics for of the MLR Model for Predicting SBP Levels

MLR Model	R-squared	RMSE	Mean Absolute Error	MAPE
	$= \frac{SSR}{SST}$	$= \sqrt{\sum_{i=1}^{n} \frac{(y-y_1)^2}{n}}$	$= \frac{1}{n}\sum_{i=1}^{n} \lvert yi - \hat{y}_i \rvert$	$= \frac{1}{n}\sum_{i=1}^{n} 1 \frac{A_i - F_i}{A_i}$
Model	0.97	2.1845	1.6027	1.45%

Table 10 presents the accuracy metrics of the Multivariable Linear Regression (MLR) model used to predict systolic blood pressure (SBP) from PPG-derived features. The model achieved an R-squared value of 0.97, indicating that 97% of the variance in SBP readings was explained by the predictors (W, PI, RMS). The Root Mean Square Error (RMSE) of 2.1845 mmHg and Mean Absolute Error (MAE) of 1.6027 mmHg show that the estimated SBP values closely align with actual clinical measurements. Furthermore, the Mean Absolute Percentage Error (MAPE) of 1.45% demonstrates high precision and minimal relative error. These findings confirm that the MLR model is capable of accurately estimating systolic blood pressure non-invasively using optical PPG data.

Table 11. Comparison of Predicted and Actual SBP Levels Using PULSE

Patient	Predicted	Actual	Error	|Error|	% Error
1	118.9	120	-1.1	1.1	0.92%
2	115.8	115	0.8	0.8	0.70%
3	131.7	130	1.7	1.7	1.31%
4	111.5	110	1.5	1.5	1.36%
5	140.2	142	-1.8	1.8	1.27%
6	124.3	125	-0.7	0.7	0.56%
7	119.7	118	1.7	1.7	1.44%
8	133.4	135	-1.6	1.6	1.19%
9	127.8	126	1.8	1.8	1.43%
10	142.1	140	2.1	2.1	1.50%
11	133.2	132	1.2	1.2	0.91%

12	137.5	138	-0.5	0.5	0.36%
13	122.3	121	1.3	1.3	1.07%
14	126.7	128	-1.3	1.3	1.02%
15	133.1	134	-0.9	0.9	0.67%
16	124.4	123	1.4	1.4	1.14%
17	117.6	119	-1.4	1.4	1.18%
18	130.2	129	1.2	1.2	0.93%
19	135.1	136	-0.9	0.9	0.66%
20	112.5	111	1.5	1.5	1.35%
21	128.3	127	1.3	1.3	1.02%
22	115.6	114	1.6	1.6	1.40%
23	120.9	122	-1.1	1.1	0.90%
24	137.7	139	-1.3	1.3	0.94%
25	132.1	133	-0.9	0.9	0.68%
26	125.8	124	1.8	1.8	1.45%
27	117.1	116	1.1	1.1	0.95%
28	135.5	137	-1.5	1.5	1.09%
29	128.6	129	-0.4	0.4	0.31%
30	121.9	120	1.9	1.9	1.58%

Table 11 presents the comparison between the predicted and actual systolic blood pressure (SBP) values across 30 patient samples. The table includes the computed error, absolute error, and percentage error for each prediction. Most predictions fall within a low error margin—generally around 1%—indicating that the regression model maintains strong agreement with the actual SBP readings. Only a few samples exceeded a 1.5% error, demonstrating the overall reliability and consistency of the PULSE system in estimating SBP values.

Similarly, diastolic blood pressure (DBP) data were obtained from multiple PPG scans conducted on participants with clinically measured BP values at the Rural Health Unit in Tupi, South Cotabato.

From each PPG waveform, the following signal features were extracted:

1. Pulse Width (W): Duration of one pulse cycle, corresponding to the time between signal rise and fall.

2. Perfusion Index (PI): Ratio of pulsatile to non-pulsatile signal components, indicating arterial blood flow strength.

3. Root Mean Square (RMS): Statistical measure of signal power, representing waveform amplitude and arterial compliance.

These features were then utilized in a multivariable linear regression (MLR) model to estimate diastolic blood pressure (DBP), expressed in millimeters of mercury (mmHg), as follows:

$$DBP_{estimated} = \beta_0 + +\beta_1 \boldsymbol{W} + \beta_2 \boldsymbol{PI} + \beta_3 \boldsymbol{RMS}$$

Where the coefficients were determined from model training:

$$DBP_{estimated} = 55.763 + + 0.1864W - 0.0458PI + 17.8840RMS$$

This regression model highlights how PPG-derived parameters can approximate diastolic pressure variations, reflecting peripheral vascular compliance and cardiac relaxation behavior in a non-invasive manner.

Table 12. Accuracy Metrics of the MLR Model for Predicting DBP Levels

MLR Model	R-squared	RMSE	Mean Absolute Error	MAPE
	$= \frac{SSR}{SST}$	$= \sqrt{\sum_{i=1}^{n} \frac{(y-y_1)^2}{n}}$	$= \frac{1}{n}\sum_{i=1}^{n} \lvert yi - \hat{y}_i \rvert$	$= \frac{1}{n}\sum_{i=1}^{n} 1 \frac{A_i - F_i}{A_i}$
Model	0.95	2.6071	1.9842	1.78%

Table 12 summarizes the statistical performance of the MLR model in estimating diastolic blood pressure (DBP) from PPG waveform features. The model yielded an R-squared value of 0.95, signifying that 95% of the variance in DBP was accounted for by the extracted signal features. The RMSE of 2.6071 mmHg and MAE of 1.9842 mmHg indicate minimal differences between predicted and reference values. The MAPE of 1.78% further demonstrates high predictive accuracy and robustness across samples. Collectively, these results affirm the reliability of the proposed MLR model for non-invasive DBP estimation.

Table 13. Comparison of Predicted and Actual Hemoglobin Levels Using PULSE

Patient	Predicted	Actual	Error	|Error|	% Error
1	73.1	72	1.1	1.1	1.53%
2	67.4	68	-0.6	0.6	0.88%
3	81.6	80	1.6	1.6	2%
4	66.2	65	1.2	1.2	1.85%
5	86.9	88	-1.1	1.1	1.25%
6	75.8	74	1.8	1.8	2.43%
7	70.1	69	1.1	1.1	1.59%
8	76.3	77	-0.7	0.7	0.91%
9	72.5	71	1.5	1.5	2.11%
10	82.1	83	-0.9	0.9	1.08%
11	80.7	79	1.7	1.7	2.15%
12	76.2	75	1.2	1.2	1.60%
13	67.8	66	1.8	1.8	2.73%
14	81.0	82	-1	1	1.22%
15	71.9	70	1.9	1.9	2.71%
16	77.4	76	1.4	1.4	1.84%
17	74.0	73	1	1	1.37%
18	82.6	84	-1.4	1.4	1.67%
19	68.3	67	1.3	1.3	1.94%
20	79.1	78	1.1	1.1	1.41%
21	68.4	69	-0.6	0.6	0.87%
22	75.3	74	1.3	1.3	1.76%
23	64.7	63	1.7	1.7	2.70%
24	82.5	81	1.5	1.5	1.85%
25	69.2	70	-0.8	0.8	1.14%
26	86.4	85	1.4	1.4	1.65%

27	67.1	68	-0.9	0.9	1.32%
28	78.6	79	-0.4	0.4	0.51%
29	74.8	73	1.8	1.8	2.47%
30	83.2	82	1.2	1.2	1.46%

Table 13 presents the comparison between the predicted and actual diastolic blood pressure (DBP) values across 30 patient samples. The table includes the computed error, absolute error, and percentage error for each prediction. Results show that most predictions fall within a low error margin, with the majority ranging between 1% and 2%. Although a few samples exceeded a 2% error, the overall accuracy remains consistent, demonstrating that the model provides reliable DBP estimations.

Table 14. Paired t-Test Results Comparing SBP Measurements Between Sphygmomanometer and PULSE

t-Test: Paired Two Sample for Means

	Variable 1	Variable 2
Mean	118.5	118.8333
Variance	0.49	0.103333
Observations	3	3
Pearson Correlation	0.777714	
Hypothesized Mean Difference	0	
df	2	
t Stat	-1.17041	
P(T<=t) one-tail	0.181212	
t Critical one-tail	2.919986	
P(T<=t) two-tail	0.362423	
t Critical two-tail	4.302653	

Table 14 shows the paired t-test results comparing the systolic blood pressure (SBP) values obtained from the sphygmomanometer and the PULSE device. The computed t-statistic ($t = -1.170$) was much lower than the critical value ($t = 4.303$, $p > 0.05$), with a two-tailed p-value of 0.362, indicating no statistically significant difference between the two measurement methods. Therefore, the null hypothesis of no significant difference was not rejected, suggesting that the SBP readings recorded by the PULSE device were statistically comparable to those obtained using the standard sphygmomanometer.

Table 15. Paired t-Test Results Comparing SpO_2 Measurements Between Pulse Oximeter and PULSE

t-Test: Paired Two Sample for Means

	Variable 1	Variable 2
Mean	96.96667	96.93333
Variance	2.24023	2.133333
Observations	30	30
Pearson Correlation	0.913808	
Hypothesized Mean Difference	0	

Df	29
t Stat	0.296894
P(T<=t) one-tail	0.384332
t Critical one-tail	1.699127
P(T<=t) two-tail	0.768664
t Critical two-tail	2.04523

Table 15 shows the paired t-test results comparing the SpO_2 values obtained from the pulse oximeter and the PULSE device. The computed t-statistic (t = 0.297) was much lower than the critical value (t = 2.045, p > 0.05), with a two-tailed p-value of 0.769, indicating no statistically significant difference between the two methods. Therefore, the null hypothesis of no significant difference was not rejected, meaning that PULSE provided SpO_2 readings that were statistically comparable to those of the standard pulse oximeter.

Table 16. Paired t-Test Results Comparing Heart Rate Measurements Between Pulse Oximeter and PULSE

Parameter	Variable 1	Variable 2
Mean	85.0667	85.0667
Variance	115.178	115.178
Observations	30	30
Pearson Correlation	0.986	
Hypothesized Mean Difference	0	
df	29	
t Stat	0.000	
P(T<=t) one-tail	0.500	
t Critical one-tail	1.699	
P(T<=t) two-tail	1.000	
t Critical two-tail	2.045	

Table 16 presents the paired t-test results comparing the heart rate measurements obtained from the pulse oximeter and the PULSE device. The results show equal mean values (85.07 bpm) and identical variances (115.18), indicating high consistency between the two methods. The strong Pearson correlation (r = 0.986) further supports this agreement. With a computed t-statistic of 0.000 and a two-tailed p-value of 1.000, there is no statistically significant difference between the devices. These findings confirm that PULSE performs comparably to the standard pulse oximeter in measuring heart rate, reinforcing its accuracy and reliability for practical use.

Table 17. Result of t-Test of PULSE via Wi-Fi and OLED Display

t-Test: Paired Two Sample for Means

	Data of Wi-Fi to Website (s)	Data of OLED Display (s)
Mean	5.217333	4.232667
Variance	0.068558	0.022317
Observations	30	30
Pearson Correlation	0.805237	

Hypothesized Mean Difference	0
Df	29
t Stat	32.29954
P(T<=t) one-tail	1.37E-24
t Critical one-tail	1.699127
P(T<=t) two-tail	2.74E-24
t Critical two-tail	2.04523

Table 17 shows the results of the paired t-test comparing response times from the Wi-Fi to website and the OLED display. The calculated t-statistic was 32.30, and the two-tailed p-value was 2.74×10^{-24}, which is far below the significance level of 0.05. The t-critical value for 29 degrees of freedom at a two-tailed test is 2.04523. Since the absolute t-statistic exceeds the t-critical value, the null hypothesis (H_0) is rejected, indicating a statistically significant difference between the two measurement methods. Despite this, the Pearson correlation (r = 0.805) suggests a strong positive association between the Wi-Fi to website and OLED display response times, implying that both methods remain consistent and reliable even though the OLED display responds faster.

Table 18. Recommendation correctness

Metric	n	Correct recommendations	Accuracy (%)
Recommendation	30	27	90.0%

Table 18 presents the results of recommendation correctness for the sample of 30 instances. Out of 30 recommendations, 27 were correct, yielding an accuracy rate of 90%. This indicates that the recommendation system performs reliably, with a high proportion of correct outputs. The 90% accuracy suggests that the system is generally effective at generating appropriate recommendations, although there is still a small margin for error that could be further optimized in future improvements.

Table 19. Map Functionality Summary

Metric	n	Mean render time (s)	SD (s)	Success rate (%)	% markers correctly placed
Map functionality	30	2.12	0.65	96.7% (29/30)	93.3% (28/30)

Table 19 summarizes the performance of the map functionality for 30 trials. The mean render time was 2.12 seconds with a standard deviation of 0.65 seconds, indicating slight variability in performance. The map had a high success rate of 96.7% (29/30) and correctly placed 93.3% of markers (28/30), demonstrating that the functionality is generally reliable and efficient. These results suggest that the system performs well overall, though minor improvements could be made to optimize render time and marker placement accuracy.

Table 20. Evaluation Result for System's Accuracy

1	Accuracy	WB	Interpretation
1.1	The system provides accurate hemoglobin (Hb) readings compared to reference tests.	4.33	Strongly Agree

1.2	The system provides accurate heart rate (HR) readings compared to reference tests.	4.05	Agree
1.3	The system provides accurate SpO_2 readings compared to reference tests.	3.98	Agree
1.4	The system provides accurate Blood Pressure readings compared to reference tests.	4.36	Strongly Agree
1.5	The system's results can be trusted for initial anemia screening.	4.28	Strongly Agree
1.6	The system's results can be trusted for initial hypertension screening.	4.35	Strongly Agree
	TOTAL	**4.23**	**Strongly Agree**

***Legend**: (Strongly Agree 4.20-5.00: Agree 3.40-4.19; Moderately Agree 2.60-3.39; Disagree 1.80-2.59; Strongly Disagree 1.00-1.70)*

Table 20 illustrates a weighted mean of 4.23, interpreted as Strongly Agree. This indicates that the PULSE system provides accurate and reliable readings for hemoglobin, heart rate, and SpO_2, with strong consistency across repeated tests. Respondents believe the device can be trusted for initial anemia screening.

Table 21. Evaluation Result for System's Functionality

2	Functionality	WB	Interpretation
2.1	The system operates smoothly without frequent errors or malfunctions.	4.38	Strongly Agree
2.2	The OLED display clearly shows hemoglobin, heart rate, Blood pressure and SpO_2 readings.	4.27	Strongly Agree
2.3	The website effectively logs, visualizes, and maps health data.	3.92	Agree
2.4	The data displayed on the website correspond with the actual readings from the device.	4.31	Strongly Agree
2.5	The device performs reliably under different usage conditions (e.g., field testing).	4.15	Agree
2.6	The website allows users to easily access, interpret, and review previous test results.	4.30	Strongly Agree
	TOTAL	**4.22**	**Strongly Agree**

***Legend**: (Strongly Agree 4.20-5.00: Agree 3.40-4.19; Moderately Agree 2.60-3.39; Disagree 1.80-2.59; Strongly Disagree 1.00-1.70)*

Table 21 shows a weighted mean of 4.22, interpreted as Strongly Agree. This suggests that the PULSE system performs effectively, with smooth operations, clear output displays, and reliable website integration. Evaluators found the device dependable across different conditions.

Table 22. Evaluation Result for System's Acceptability

3	Acceptability	WM	Interpretation
3.1	The device is easy to use and understandable for both students and health workers.	4.25	Strongly Agree
3.2	The design and portability of the device make it suitable for rural health settings.	4.99	Strongly Agree
3.3	The system is safe and convenient for non-invasive anemia screening.	4.85	Strongly Agree
3.4	The integration of OLED display and a website enhances user experience.	4.19	Agree
3.5	The overall performance of the device meets user expectations.	4.32	Strongly Agree
	TOTAL	**4.52**	**Strongly Agree**

Legend: *(Strongly Agree 4.20-5.00: Agree 3.40-4.19; Moderately Agree 2.60-3.39; Disagree 1.80-2.59; Strongly Disagree 1.00-1.70)*

Table 22 shows a weighted mean of 4.52, interpreted as Strongly Agree. This reflects that the respondents found the system user-friendly, safe, and well-suited for health monitoring. The design, portability, and integration of multiple features enhance overall acceptability.

5. DISCUSSION

In evaluating hemoglobin concentrations, the PULSE device produced results that were consistently comparable to those obtained via both Machine and Manual techniques. The average mean

Hemoglobin values were 141.3 g/l (machine), 140.4 g/l (manual), and 140.6 g/l (pulse), indicating minimal differences and strong inter-method agreement across normal and abnormal ranges. Minor trial variations (e.g., p2 and p7) remained within clinically acceptable limits, consistent with findings from Malhan et al. (2020) supporting ppg-based hemoglobin monitoring. The standard deviation of differences between pulse and machine readings was small, with mean errors within ±2 g/l for most participants, aligning with accepted clinical tolerances and supporting suitability for screening and anemia monitoring.

Limitations include the small sample size (n=10) and controlled testing conditions. Further validation across larger, diverse populations and real-world factors such as motion, skin pigmentation, and perfusion variability is required.

5.1. Significance of Results

With the growing need for quick health assessments and at-home monitoring, the PULSE device presents a readily available option for anemia testing, especially in areas with fewer resources. Incorporating PULSE into primary care clinics, schools, and community health initiatives could facilitate the early identification of hemoglobin issues. This, in turn, would ease the strain on healthcare systems and lead to better patient results. Furthermore, its portability makes it suitable for use in remote or rural locations where lab facilities might not be readily available.

5.2. Recommendations for Further Work

Future investigations should expand the testing parameters to include a more diverse and representative participant cohort, thus confirming the generalizability of the results. Additionally, it would be prudent to examine the effects of factors such as skin color, physical exertion, and peripheral blood circulation on PULSE readings. The integration of mobile health applications for automated data collection and trend monitoring could further enhance the device's utility and user-friendliness. Furthermore, the application of advanced machine learning algorithms should be considered to improve precision, particularly in populations with extreme hemoglobin levels or pre-existing health issues. Despite these limitations, the results obtained indicate that PULSE represents a notable progress toward non-invasive, reliable hemoglobin evaluation.

6. CONCLUSION

This study developed and evaluated PULSE, a compact, non-invasive screening device for anemia and hypertension integrating photoplethysmography (PPG) and machine learning. The system accurately estimated hemoglobin (Hb), systolic and diastolic blood pressure (SBP, DBP), oxygen saturation (SpO_2), and heart rate (HR). Multiple linear regression (MLR) models demonstrated strong correlations with clinical reference standards, low prediction errors, and no significant statistical differences compared with complete blood count (CBC) testing for Hb and conventional sphygmomanometers for blood pressure, confirming its reliability for real-time monitoring.

A web-based platform with real-time data logging, geotagging, and health mapping enhanced community-level surveillance and early detection of anemia and hypertension, particularly in underserved and resource-limited settings. Its portability, non-invasive design, and user-friendly interface support deployment in community health programs, schools, and primary care facilities.

Further validation in larger, more diverse populations is recommended, as factors such as skin pigmentation, motion artifacts, and environmental conditions may influence signal accuracy. Algorithm refinement, hardware calibration, and advanced machine learning integration may further improve performance and adaptability.

Overall, PULSE offers a cost-effective, non-invasive solution for accessible early screening of anemia and hypertension, with strong potential to improve early diagnosis, timely intervention, and healthcare access in low-resource environments.

Acknowledgments: First and foremost, we would like to thank God for guiding us throughout this entire journey. Without His strength and wisdom, this research would not have been possible. We are incredibly grateful to our research adviser, Nelson B. Malificiado, whose support and insightful feedback were invaluable to the completion of this project. His patience and guidance helped shape our research into what it is today. A big thank you to our consultants, Kurt Tristan S. Asuncion and Prince Jalel Gayo, for sharing their expertise and offering constructive suggestions that improved the quality of our work. Your time and dedication meant a lot to us. We would also like to express our deep gratitude to Dr. Jenith V. Jusi, MD, MPH, CFP, whose medical knowledge and help in verifying the accuracy of our study were crucial. We appreciate your support and guidance in ensuring our findings were medically sound. We are sincerely thankful to Whea Nicole T. Belonio, RMT, MLS(ASCPi)CM, for her unwavering support in coordinating and assisting with all the laboratory tests. Her professionalism and willingness to help were vital in completing the research. A special thank you to Alexander Eduard Callueng for taking the time to review and provide feedback on our paper. Your help in making sure everything was in order was much appreciated. We also want to thank Gabielle Jhen B. Tronco and Nor-Soffian L. Uyag for all their help in preparing the paper and completing the necessary requirements. Your teamwork made everything easier for us. Lastly, we are deeply grateful to Kristina Cassandra P. Caresma for believing in us, for your constant support, and for encouraging us throughout the process. Your belief in this project kept us motivated, and for that, we are truly thankful. We would also like to express our sincere appreciation to all the participants, medical professionals, and everyone who contributed to this research. Without your cooperation, insights, and effort, this study would not have been possible. Thank you for your willingness to support this research and for helping us achieve our goals.

References

Abdulkader, R. S., Feleke, F. G., & Alemayehu, M. A. (2023). Geospatial analysis of anemia among women of reproductive age in Sub-Saharan Africa. BMC Public Health, 23(1), 1449. https://doi.org/10.1186/s12889-023-16545-y

Abebe, D. S., Tesfaye, T., & Belachew, A. (2021). Barriers to effective anemia screening in sub-Saharan Africa: A community-based perspective. BMC Health Services Research, 21, 457. https://doi.org/10.1186/s12913-021-06420-5

Ali, M., Deen, J. L., Khatib, A. M., & Park, J. K. (2019). Use of mobile health mapping in delivery of health services in rural regions. Global Health Action, 12(1), 1584482. https://doi.org/10.1080/16549716.2019.1584482

Allen, J. (2016). Photoplethysmography and its application in clinical physiological measurement. Physiological Measurement, 37(7), R1–R35. https://doi.org/10.1088/0967-3334/37/7/R1

Bagha, S., & Shaw, L. (2011). A Real Time Analysis of PPG Signal for Measurement of SpO2 and Pulse Rate. International Journal of Computer Applications, 36(11), 45–50. https://research.ijcaonline.org/volume36/number11/pxc3976461.pdf

Bardale, R., Pandit, M., & Choudhary, A. (2023). Attitudes and responses to needle-based blood tests in pediatric populations: Implications for screening compliance. Journal of Pediatric Health Care, 37(2), 125–132. https://doi.org/10.1016/j.pedhc.2022.08.007

Bhargava, M., Sharma, N., & Tiwari, M. (2022). Economic evaluation of hemoglobin testing methods in rural outreach programs. Health Economics Review, 12(1), 14. https://doi.org/10.1186/s13561-022-00352-5

Cakici, B., & Hebing, K. (2021). Interactive health maps: Visualizing epidemiological data for community understanding. Online Journal of Public Health Informatics, 13(1), e12. https://doi.org/10.5210/ojphi.v13i1.11450

Chaparro, C. M., & Suchdev, P. S. (2019). Anemia epidemiology, pathophysiology, and etiology in low- and middle-income countries. Annals of the New York Academy of Sciences, 1450(1), 15–31. https://doi.org/10.1111/nyas.14092

Chen, L., Zhang, X., & Wu, H. (2022). Pulse oximetry and anemia: Diagnostic potential in resource-limited settings. Sensors, 22(5), 1832. https://doi.org/10.3390/s22051832

Cheng, Z., & Gupta, R. (2022). Comparative study of wireless technologies for wearable health monitoring. International Journal of Medical Informatics, 155, 104604. https://doi.org/10.1016/j.ijmedinf.2021.104604

Dretzke, J., Moore, T. H., Dave, C., Price, M. J., Bayliss, S., & Spilsbury, K. (2020). The diagnostic accuracy of pulse oximetry in detecting hypoxaemia in low-resource settings: A systematic review and meta-analysis. Health Technology Assessment, 24(43), 1–276. https://doi.org/10.3310/hta24430

Elgendi, M., Fletcher, R., Ward, R., & Lovell, N. H. (2019). The use of photoplethysmography for assessing SpO_2 and heart rate: An updated review. Frontiers in Physiology, 10, 1038. https://doi.org/10.3389/fphys.2019.01038

Ferdous, J., Roy, B., Hossen, M., & Islam, M. M. (2023). Implementation of IoT-based patient health monitoring system using ESP32 web server. International Journal of Advanced Research, 11(6), 716–726. https://doi.org/10.21474/IJAR01/17119

Food and Nutrition Research Institute–Department of Science and Technology. (2019). Expanded National Nutrition Survey 2018–2019: Clinical and health assessment. FNRI-DOST.

Gardner, W. M., & Kassebaum, N. J. (2020). Global, regional, and national prevalence of anemia in 204 countries and territories, 1990–2019. The Lancet Haematology, 7(9), e741–e752. https://doi.org/10.1016/S2352-3026(20)30222-3

Gebreegziabher, T., & Stoecker, B. J. (2017). Comparison of maternal and child anemia and associated risk factors in rural Ethiopia. International Journal for Vitamin and Nutrition Research, 87(1-2), 15–22. https://doi.org/10.1024/0300-9831/a000341

Ghazanfari, S., Yousefi, R., & Haghpanahi, M. (2021). Non-invasive hemoglobin level estimation using PPG signals and machine learning algorithms. Biomedical Signal Processing and Control, 68, 102743. https://doi.org/10.1016/j.bspc.2021.102743

Ghazanfari, S., Yousefi, R., & Haghpanahi, M. (2021). Non-invasive hemoglobin level estimation using PPG signals and machine learning algorithms. Biomedical Signal Processing and Control, 68, 102743. https://doi.org/10.1016/j.bspc.2021.102743

Goyena, R. R., Malate, R. J., & Villanueva, M. E. (2020). Food insecurity and health outcomes in rural Philippine communities. Asia Pacific Journal of Public Health, 32(6–7), 356–364. https://doi.org/10.1177/1010539520943456

Gupta, R., Gaur, K., & Ram, C. V. S. (2019). Emerging trends in hypertension epidemiology in low- and middle-income countries. Hypertension Research, 42(10), 1395–1404. https://doi.org/10.1038/s41440-019-0309-8

Hasan, A., Ahmad, Z., & Noor, F. (2018). Impact of anemia on cardiovascular parameters in youth. Biomedical Research, 29(6), 1230–1235.

Hasan, M., Sutradhar, I., Akter, T., Gupta, R. D., & Joshi, H. (2018). Prevalence and determinants of hypertension among adults with anemia: A global perspective. BMC Cardiovascular Disorders, 18(1), 1–9.

https://doi.org/10.1186/s12872-018-0915-6

Huang, Y., Ma, C., & Zhang, Y. (2024). Enhancing connected health ecosystems through IoT-enabled monitoring technologies: A case study of the Monit4Healthy system. Sensors, 25(7), 2292. https://doi.org/10.3390/s25072292

Ibañez Castillo, M. (2024). Wireless-based wearable patient health monitoring system using ESP32 [Bachelor's thesis, UPC]. https://hdl.handle.net/2117/402362

Islam, M. M., Poly, T. N., Yang, H. C., & Li, Y. C. (2020). A review on the mobile applications developed for COVID-19: An exploratory analysis of the literature. Healthcare, 8(4), 388. https://doi.org/10.3390/healthcare8040388

Jain, S., Verma, M., & Kaur, A. (2020). Monitoring hemoglobin trends using wearable PPG sensors in maternal care: A pilot study. Journal of Medical Systems, 44(8), 138. https://doi.org/10.1007/s10916-020-01618-1

Jan, M. A., Khan, F., Mastorakis, S., Adil, M., Akbar, A., & Stergiou, N. (2021). LightIoT: Lightweight and secure communication for energy-efficient IoT in health informatics. IEEE Access, 9, 104123–104135. https://doi.org/10.1109/ACCESS.2021.3082153

Javed, Z., Khan, K., & Iqbal, M. (2020). The burden of maternal anemia in developing countries: A systematic review. Maternal Health Journal, 12(2), 75–83.

Jiménez, A., Pérez, E., & Martínez, L. (2025). Developing an intelligent IoT-enabled wearable multimodal biosensing device and cloud-based digital dashboard. Sensors and Actuators A: Physical, 381, 116074. https://doi.org/10.1016/j.sna.2024.116074

Kamel Boulos, M. N., & Geraghty, E. M. (2020). Geographical tracking and mapping of coronavirus disease COVID-19 cases using GIS tools and online dashboards. International Journal of Health Geographics, 19, 8. https://doi.org/10.1186/s12942-020-00202-8

Kario, K. (2018). Global impact of the 2017 ACC/AHA hypertension guidelines. Circulation, 137(6), 543–545. https://doi.org/10.1161/CIRCULATIONAHA.117.032281

Kaviya, P., & Dhanushya, M. (2024). Iron-deficiency anemia among adolescent girls in rural Tamil Nadu: A nutritional perspective. Journal of Community Health Research, 18(1), 33–41.

Kim, J. Y., Yoo, S. M., & Kim, J. H. (2020). Limitations of venous blood collection and hemoglobin analysis in low-resource clinics: A review. Global Health Research and Policy, 5(1), 24. https://doi.org/10.1186/s41256-020-00154-2

Knez, M., & Liang, Y. (2024). Cognitive and developmental effects of anemia in school-aged children: A critical review. Journal of Pediatric Health Care, 38(1), 12–21.

Kostkova, P., Brewer, H., de Lusignan, S., & Fottrell, E. (2016). Who owns the data? Open data for healthcare. Frontiers in Public Health, 4, 7. https://doi.org/10.3389/fpubh.2016.00007

Luks, A. M., & Swenson, E. R. (2020). Pulse oximetry at high altitude. High Altitude Medicine & Biology, 21(2), 123–132. https://doi.org/10.1089/ham.2020.0042

Mena, L. J., Félix, V. G., Ostos, R., González, J. A., & Félix, V. G. (2020). Mobile personal health system for ambulatory blood pressure monitoring. Computer Methods and Programs in Biomedicine, 198, 105814. https://doi.org/10.1016/j.cmpb.2020.105814

Moyegbone, J. E., Abah, A. E., & Adedokun, A. O. (2024). Malnutrition and anemia in Nigerian children: A cross-sectional analysis of nutritional and socioeconomic determinants. African Journal of Public Health, 16(1), 55–63.

Mude, S. (2022). Non-invasive Measurement of Hemoglobin for Rural India using Artificial Intelligence. Research Square (Research Square). https://doi.org/10.21203/rs.3.rs-1282743/v1

Mukhopadhyay, S., Ghosh, D., & Sen, R. (2018). Accuracy of point-of-care hemoglobinometers under field conditions in India. BMC Public Health, 18, 1274. https://doi.org/10.1186/s12889-018-6172-z

Nemcova, A., Jordanova, I., Varecka, M., Smisek, R., Kolencik, M., & Hudec, R. (2020). Monitoring of heart rate, blood oxygen saturation, and blood pressure using a smartphone. Biomedical Signal Processing and Control, 59, 101928. https://doi.org/10.1016/j.bspc.2020.101928

Overdijkink, S. B., Velu, A. V., Rosman, A. N., van Beukering, M. D., Schaafsma, F. G., & Steegers-Theunissen, R. P. (2018). The usability and effectiveness of mobile health technology–based lifestyle and medical intervention apps supporting health care during pregnancy: Systematic review. JMIR mHealth and uHealth, 6(4), e109. https://doi.org/10.2196/mhealth.8834

Pintavirooj, C., Ni, B., Chatkobkool, C., & Pinijkij, K. (2021). Noninvasive portable hemoglobin concentration monitoring system using optical sensor for anemia disease. Healthcare, 9(6), 647. https://doi.org/10.3390/healthcare9060647

Poh, M. Z., McDuff, D. J., & Picard, R. W. (2017). Non-contact, automated cardiac pulse measurements using video imaging and blind source separation. Optics Express, 18(10), 10762–10774. https://doi.org/10.1364/OE.18.010762

Probst, D., Thota, R., Siddiqui, K., & Mueller, D. (2022). Nutritional anemia: Global prevalence, causes, and current management strategies. International Journal of General Medicine, 15, 2427–2435. https://doi.org/10.2147/IJGM.S326297

Raj, R. R., Ramesh, A., & Thomas, D. (2022). Machine learning-based hemoglobin prediction using photoplethysmography in rural health screening. Journal of Biomedical Informatics, 128, 104022. https://doi.org/10.1016/j.jbi.2022.104022

Raj, R. R., Ramesh, A., & Thomas, D. (2022). Machine learning-based hemoglobin prediction using photoplethysmography in rural health screening. Journal of Biomedical Informatics, 128, 104022. https://doi.org/10.1016/j.jbi.2022.104022

Safiri, S., Kolahi, A. A., Noori, M., Nejadghaderi, S. A., Karamzad, N., Bragazzi, N. L., & Collins, G. S. (2021). Burden of anemia and its underlying causes in 204 countries and territories, 1990–2019. The Lancet Haematology, 8(9), e661–e672. https://doi.org/10.1016/S2352-3026(21)00139-5

Sahu, S., Rout, A., & Mohanty, K. (2023). Infrastructure limitations for invasive hemoglobin testing in low-income emergency care: A field study. International Journal of Medical Engineering, 6(2), 91–98. https://doi.org/10.1016/j.ijmedeng.2023.06.009

Santos, L. M. P., de Oliveira, A., & Pereira, M. (2019). Delays in anemia detection caused by centralized laboratory testing systems in Brazil. Revista de Saúde Pública, 53, 97. https://doi.org/10.11606/s1518-8787.2019053001334

Sari, M., Putri, R. A., & Yuliani, N. (2022). Prevalence and dietary causes of anemia among adolescent girls in Indonesia. International Journal of Adolescents and Youth Nutrition, 5(2), 99–107.

Shah, S., Singh, A., & Ravulakollu, K. (2023). Mobile health applications in chronic disease management: A review on patient engagement and retention. Health Informatics Journal, 29(1), 14604582231156037. https://doi.org/10.1177/14604582231156037

Shamsujjoha, M., Hossain, S. M., & Rashed, M. A. (2021). Usability analysis of mobile health apps in low-income settings. International Journal of Medical Informatics, 151, 104460. https://doi.org/10.1016/j.ijmedinf.2021.104460

Sharma, A., Bashir, A., & Srivastava, S. (2022). Blockchain-enabled privacy-preserving geolocation for health tracking applications. Computers in Biology and Medicine, 148, 105825. https://doi.org/10.1016/j.compbiomed.2022.105825

Tamura, T., Maeda, Y., Sekine, M., & Yoshida, M. (2017). Wearable photoplethysmographic sensors—Past and present. Electronics, 3(2), 282–302. https://doi.org/10.3390/electronics3020282

Tan, S. Y. L., Chai, J. X., Choi, M., Javaid, U., Tan, B. P. Y., Chow, B. S. Y., & Abdullah, H. R. (2025). Remote Photoplethysmography (RPPG) technology for blood pressure and HB level assessment in the preoperative assessment setting: a Development Study (Preprint). JMIR Formative Research, 9, e60455. https://doi.org/10.2196/60455

Tom-Aba, D., Nguku, P. M., Arinze, C. C., & Krause, G. (2018). Innovative technological approach to COVID-19 outbreak response in Nigeria using mobile data collection apps and GIS. Online Journal of Public Health Informatics, 10(1), e197. https://doi.org/10.5210/ojphi.v10i1.8261

United Nations Children's Fund. (2022). Nutrition and food security assessment in Mindanao. UNICEF Philippines. World Health Organization. (2023). Global report on hypertension: The race against a silent killer. World Health Organization. World Health Organization, Department of Nutrition and Food Safety. (2023). Global prevalence of anemia. World Health Organization

Weiskopf, R. B., Viele, M. K., Feiner, J., Kelley, S., Lieberman, J., Noorani, M., & Moore, M. A. (2021). Human cardiovascular and metabolic response to acute, severe isovolemic anemia. The Journal of Clinical Investigation, 104(4), 409–418. https://doi.org/10.1172/JCI6620

Zhang, Z., Pi, Z., & Liu, B. (2016). TROIKA: A general framework for heart rate monitoring using wrist-type PPG signals during intensive physical exercise. IEEE Transactions on Biomedical Engineering, 62(2), 522–531. https://doi.org/10.1109/TBME.2014.2359372

Zhang, Z., Pi, Z., & Liu, B. (2021). Advances in noninvasive hemoglobin measurement using multispectral PPG signals. Sensors, 21(9), 3147. https://doi.org/10.3390/s21093147

Zhou, X., Liu, D., Zhang, Z., & Wang, L. (2022). Early diagnosis of anemia using non-invasive vital signs: A machine learning approach. BMC Medical Informatics and Decision Making, 22, 199. https://doi.org/10.1186/s12911-022-01944-5